ROYAL HOLLOWAY AND BEDFORD NEW COLLEGE
UNIVERSITY OF LONDON

DIELECTRIC SPECTROSCOPY OF SEMICONDUCTORS

5th Progress Report to July 1989
on work under US Army Grant DAJA 45-87-C-0011

Professor Andrew K Jonscher
Dr Mohammad A Bari
Mr Najeeb Siddiqui

ABSTRACT

Our understanding of the frequency dependence of transport in a two-dimensional electron gas (2-DEG) as seen in a nearly-cut-off Field-Effect Transistor (FET) is now reasonably complete, our earlier difficulties having been due to confusing experimental artefacts. The result is a confirmation of our prediction that 2-DEG should show strong Low-Frequency Dispersion (LFD), which has some fundamental significance.

We are expanding our studies to the investigation of the decay of photo-voltages in p–n junctions on high-resistivity silicon, the dielectric spectra of which were described in the 3rd Progress Report. We believe that the results will be of some interest for the better understanding of the recombination processes in these devices.

The new many-body theory of the fractional power-law time-dependence of trapping/generation processes in deep levels in space charge regions of p-n junctions and Schottky barriers has now been accepted by Solid State Electronics. This theory departs radically from previously accepted interpretations which predict near-exponential decay, while our experimental evidence shows that this is only a limiting case of a much more general form of dependence. (AW)

2-DIMENSIONAL ELECTRON GAS

Our interest in the transport properties of 2-dimensional electron gas (2-DEG) was aroused by our earlier discovery in the context of studies of transport on humid insulators that such 2-D transport shows both *spatial* non-uniformity in the form of *filamentation* and also strong Low-Frequency Dispersion (LFD) [1]. The latter manifests itself [2] by strongly dispersive real and imaginary components of the capacitive equivalent of the complex dielectric susceptibility:

$$\chi(\omega) \equiv C(\omega) - C_\infty = \chi'(\omega) - i\chi''(\omega) \propto (i\omega)^{n-1} \qquad (1)$$

where $C(\omega)$ is the complex capacitance and C_∞ is its "high-frequency" limit. The exponent n in this relation is small compared to unity, giving strong dispersion, together with the property that the ratio

$$\chi''(\omega)/\chi'(\omega) = \cot(n\pi/2) \qquad (2)$$

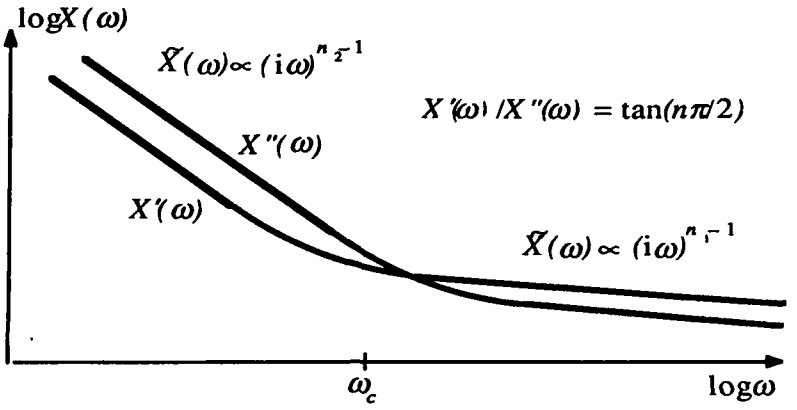

Figure 1. The frequency dependence of the real and imaginary components of the complex dielectric susceptibility of a system showing "normal" dielectric behaviour at higher frequencies and Low-Frequency Dispersion at lower frequencies. Both follow the "universal" form of fractional power laws with, respectively, large and small values of the exponent n.

is independent of frequency – this is a general property of the "universal" dielectric relation [2]. With LFD this ratio is larger than one, the system is very lossy, while for more conventional dielectric responses $n \approx 1$ and the losses are low. This type of behaviour is shown schematical in Figure 1. In the LFD system there is a large accumulation of charge at low frequencies and the significance of this is understood in ionic systems [3] but its interpretation in electronic transport is rather difficult at present.

It is instructive to look at the alternating-current (ac) conductance corresponding to LFD, which is given by:

$$G(\omega) = \omega X''(\omega) \propto \omega^{n} \tag{3}$$

which corresponds to a very slowly frequency-dependent conductance, as shown in Figure 2.

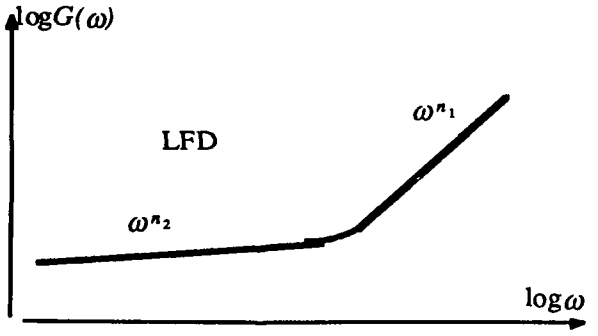

Figure 2. A schematic representation of the frequency dependence of the ac conductance $G(\omega)$ which in the LFD mode corresponds to a very slowly frequency-varying conductance, closely approaching dc conductance, except for the strongly dispersive $C'(\omega)$. The high-frequency part corresponds to the usual dielectric behaviour.

The fundamental difference between the LFD behaviour and conventional direct–current (dc) conductance G_0 lies in the fact that for dc the exponent $n = 0$ and the real part $X'(\omega) \equiv 0$. The relationship between the charging and discharging currents in LFD is further discussed in [4].

The importance of the discovery of LFD in 2-DEG lies in the fact that it extends the range of applicability of this form of transport from ionic systems to purely electronic ones and this is of considerable fundamental significance for the understanding of the dynamics of low-dimensional flow.

Our work on FETs in nearly-cut-off condition reported earlier had been confused by certain experimental artefacts which made it difficult to distinguish clearly between the LFD processes in question and the effect of the distributed *R–C* line which is formed between the channel and the substrate and gate of the FET and which leads to a "diffusive" law with $n = 1/2$, as discussed in the Appendix. We have seen the LFD response [3] but it was difficult to understand some of the complications in the experimental picture. We have now succeeded in clarifying the position, among other points by running the FET at 70° C.

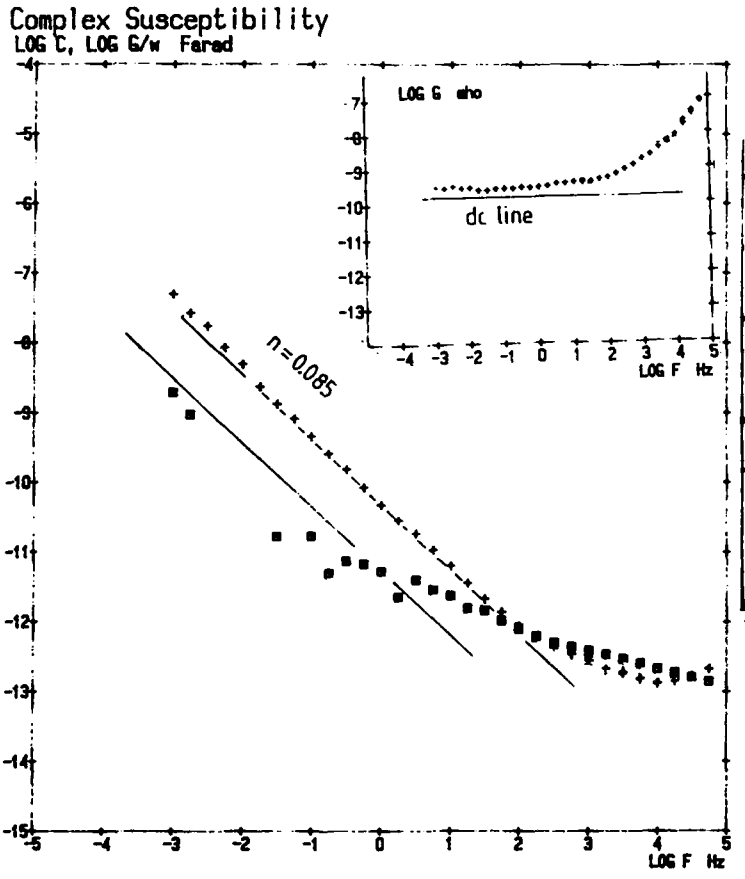

Figure 3. The frequency dependence of the dielectric susceptibility of a nearly-cut-off FET at 70°C . The inset shows the corresponding ac conductance. The sloping lines are drawn in Kramers-Kronig–compatible positions, showing the self–consistency of the results. The LFD region is clearly seen, with a variation of $X'(\omega)$ by more than two orders of magnitude above C_∞. At the higher frequencies we have a region with $n \approx 0.5$.

The experimental results are shown in Figure 3 as $X'(\omega)$ and $X''(\omega)$ which clearly reveals the LFD region and the high-frequency part which follows a power law with $n \approx 0.5$, in agreement with eqn (A5).

These results show beyond doubt the existence of LFD in a 2-DEG and the full significance of this result will have to be explored in the future - the most important questions being the correlation between the LFD and the geometry of the channel and also the density of 2-DEG which is governed by the bias applied to the gate.

The theory of ac conduction in FETs is given in the Appendix.

DECAY OF PHOTOVOLTAGE IN JUNCTION DIODES

An open-circuited p-n junction under illumination by light of greater-than-bandwidth quantum energy causes an effective forward biasing of the junction which is required to balance the photocurrent that would otherwise be flowing in the diode. Since a forward current is given by the usual expression

$$i = A \exp(eV/\alpha kT) \propto \Delta n_0 \qquad (4)$$

where A is a constant and α is the "ideality factor" which is usually of the order of 2. Δn_0 is the boundary excess density of charge carriers due to light excitation. Consequently, the open-circuit photovoltage is given from eqn (4) by:

$$V_\phi = \alpha kT \ln(\Delta n_0) \qquad (5)$$

suggesting that the *linear* photovoltage gives a *logarithmic* plot of the excess carrier density. By measuring the linear time dependence of V_ϕ we are able to obtain the deviations from the expected simple *exponential* time decay as deviations from straight line response.

Figure 4 shows the dependence of the photovoltage for two experimental conditions, all at room temperature.The linear time base runs to 10 ms and the V_ϕ scale is marked directly in units of 0.1V volts. Data a) give the zero line, b) the response to a short flash with zero bias, c) is the a steady forward bias of 0.1V without flash and d)corresponds to the superpositon of flash on c). e) and f) are four-fold expanded plots of the later stages of b) and d), respectively, with the limiting steady state lines drawn in correct positions.

It is evident that the decay deviates from a straight line dependence, with a cusp appearing after some 2 ms and a much longer tail setting in for 3-4 ms, which may or may not be linear. The decay of V_ϕ in the presence of background illumination is much slower and we will need to follow the decay on a longer time scale.

We are not at present in position to determine with any assurance what are the respective contributions to the non-exponential decay of the actual decay of Δn_0 and what is due to the breakdown of the simple relation (4) - this remains to be investigated. For the present, it is sufficient to have shown that these deviations exist and that we are able to measure them reliably.

We shall extend these measurements to try to establish a correlation between the photodecay and the dark frequency dependence of the complex capacitance of the respective diodes.We know that different diodes have different photodecay spectra and this should form a fruitful line of investigation, since similar trapping processes should be involved.

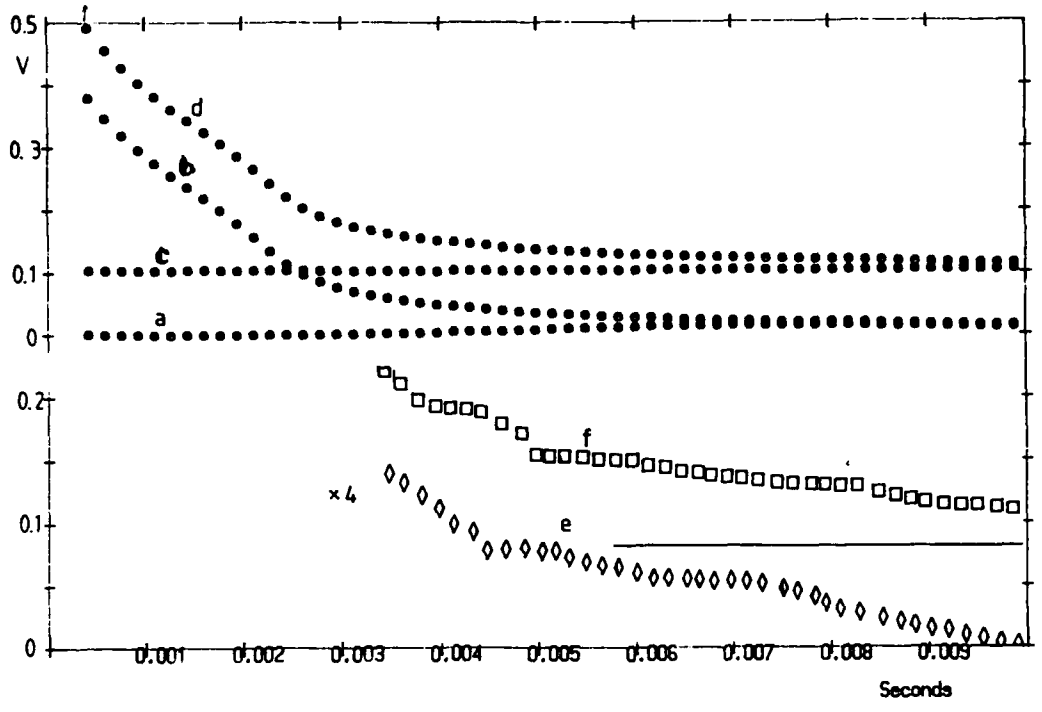

Figure 4. The decay of the open-circuit photovoltage of an implanted diode after illumination with a 1 μs flash. Trace a) corresponds to zero line, b) is the response to flash, c) is the forward bias line for 0.1V, d) gives flash superimposed on 0.1V bias. Traces e) and f) give the same results as b) and d) at later times expanded four-fold, with the corresponding steady-state lines drawn to show the long-time decay. There are clear deviations from straight line, i.e. exponential decay, and at least two very different time constants may be discerned.

References

1. E F Owede and A K Jonscher, J Electrochemical Soc **135**, 1757, 1988
2. A K Jonscher *Dielectric Relaxation in Solids*, Chelsea Dielectrics Press, London, 1983
3. A K Jonscher, 1988 Annual Report, Conference on Electrical Insulation and Dielectric Phenomena, Ottawa, IEEE Insulation Society, p 190.
4. A K Jonscher and T Ramdeen, IEEE Transactions **EI-22**, 35-39, 1987

Acknowledgements

It is a pleasure to acknowledge the help of Dr T P L Li of Martin Marietta Electronic Systems, Orlando, FL and of Mr D H J Totterdell of Harwell Laboratory of the UK Atomic Energy Authority, who kindly supplied samples of long-lifetime diodes on high-resistivity silicon.

Appendix

Analysis of MOST channel response under alternating voltage

We are proposing to derive the frequency dependence of the channel admittance on the basis of the geometrical diagram shown in Figure 5a) and of the equivalent circuit shown in Figure 5b). The channel length is L and its width W, the gate - substrate bias is V_{GS} and the drain-source bias V_{DS} is sufficiently small to give a uniform field and uniform carrier density along the channel. The channel has a uniform distributed capacitance to the gate c_g per unit length and to the substrate c_s. Because the source and substrate are at the same potential the two capacitances are connected effectively in parallel and the simplified diagram of Figure 5c) applies, with the distributed capacitance $c = c_g + c_s$.

The equations of the alternating current and voltage along the length of the channel may be written in the form:

$$dV/dx = -ir \qquad di/dx = -i\omega cV \tag{A1}$$

where $i = (-1)^{1/2}$, from which follows

$$d^2V/dx^2 = s^2V \qquad \text{where} \quad s^2 = i\omega cr = i\omega C_g R_c/L^2 = i\omega\tau/L^2$$

where the time constant $\tau = C_g R_c$, leading to a solution of the form

$$V(x) = Ae^{sx} + Be^{-sx} \tag{A2}$$

and from (A1):

$$i(x) = -(s/r)\,(Ae^{sx} - Be^{-sx}) \tag{A3}$$

At the drain end, $x = 0$, $V = V_o = A + B$, while at the source end, $x = L$ the ac voltage is zero, so that with both conditions we have at the drain end

$$V_o = A(1 - e^{-2sL}) \qquad i_o = V_o\,(s/r)\coth(i\omega\tau)^{1/2} \tag{A4}$$

with the channel impedance being given by

$$Y(\omega) = i_o/V_o = (s/r)\coth(i\omega\tau)^{1/2} = i^{1/2}\,(\omega C_g R_c)^{1/2}\coth(i\omega\tau)^{1/2} \tag{A5}$$

We are interested in two types of solution, one for "short" channel, $|sL| = \omega\tau \ll 1$, the other for "long" channel, $\omega\tau \gg 1$. These conditions depend on the physical length L of the channel as well as on the specific channel resistance r which depends strongly on V_{GS}. In the short channel or low-frequency limit we have the evident result

$$Y(\omega) \approx 1/R_c \tag{A6}$$

which implies that, to the extent to which R_c is independent of frequency, the admittance is purely real and is equal to the reciprocal resistance of the channel.

The long channel or high-frequency limit limit of eqn (A5) gives

$$Y(\omega) \approx i^{1/2}\,(\omega C_g/R_c)^{1/2} = (1 + i)/2\;\omega^{1/2}\,(C_g/R_c)^{1/2} \tag{A7}$$

which is the classical Warburg diffusive law applicable to an infinitely long R–C line, in which

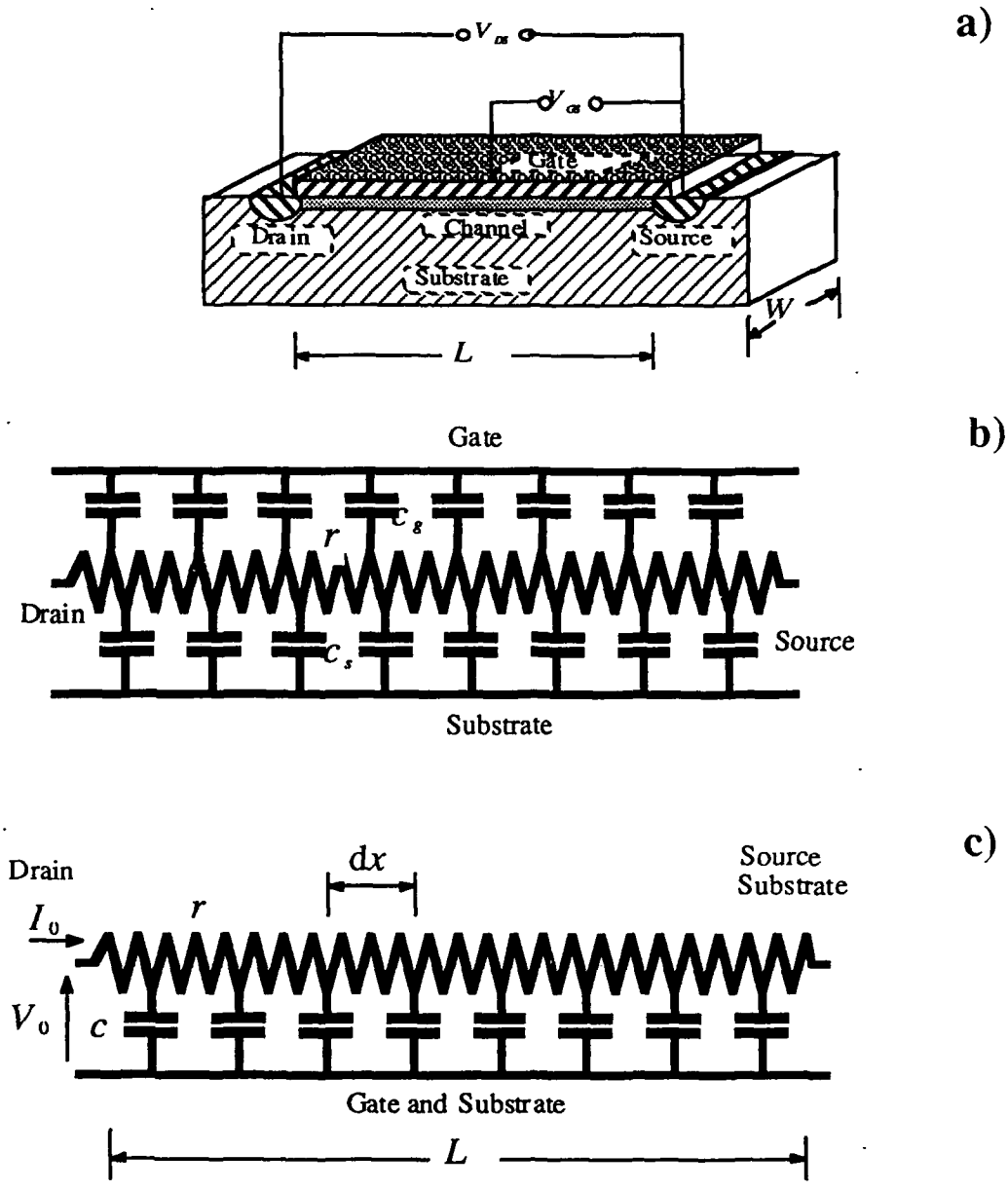

Figure 5. Diagram a) shows the physical layout of a MOST with its channel of length L between drain and source electrodes and with the gate electrode. The width of the device in the nrmal direction is W and the biasing voltages V_{GS} and V_{DS} are indicated. The source and substrate are at the same potential. Diagram b) shows the equivalent circuit of the channel which is represented by a resistance r per unit length with distributed capacitances c_g and c_s to the gate and substrate, respectively, both of which may be regarded as equipotential. All quantities r, c_s and c_g are taken for the entire width W. Diagram c) shows the equivalent circuit of the system obtained by joining the gate and substrate as one for the purpose of the alternating signal and regarding the source end as short-circuited to the substrate. The effective capacitance per unit length is $c = c_s + c_g$.

account in our analysis and this arises when the channel is completely "cut off" with $R \rightarrow \infty$, for which eqn (10) gives zero contribution to the admittance, while in real situations one obtains a response characteristic of the space charge region behaving as a low-loss dielectric in which $X'(\omega) \gg X''(\omega)$ and both are virtually independent of frequency (Jonscher 1983), implying that the conductance is very low and almost proportional to ω.